ZrNbCuNiAl bulk metallic glass matrix composites containing dendritic bcc phase precipitates

U. Kühn,[a] J. Eckert, N. Mattern, and L. Schultz
IFW Dresden, Postfach 270016, D-01171 Dresden, Germany

(Received 20 August 2001; accepted for publication 5 February 2002)

We report on phase formation of a multicomponent $Zr_{66.4}Nb_{6.4}Cu_{10.5}Ni_{8.7}Al_8$ glass-forming alloy upon copper mold casting. A bcc phase embedded in a glassy matrix forms for moldcast bulk samples yielding an *in-situ* bulk metallic glass matrix composite upon slow cooling from the melt. Upon annealing, the first exothermic transformation of the material is related to precipitation of an icosahedral phase from the glassy matrix. The formation of the bcc phase-containing metallic glass composite is strongly governed by the alloy composition and the actual cooling rate during solidification. Room-temperature compression tests reveal significant yielding and plastic deformation before failure. © *2002 American Institute of Physics.* [DOI: 10.1063/1.1467707]

Multicomponent Zr-based alloys are known for their excellent glass-forming ability.[1,2] They can be produced as bulk samples at cooling rates as low as 1–10 K/s for several alloy systems such as Zr–Ti–Cu–Ni–Be,[2] Zr–Ti–Cu–Ni–Al[3] and Zr–Nb–Cu–Ni–Al.[4] The Zr-based bulk glasses have some advantages compared to crystalline alloys of same composition, e.g., better electrochemical behavior[5] and outstanding mechanical properties, such as high yield strength of up to 2 GPa combined with an elastic strain limit of about 2%.[6] However, bulk metallic glasses and alloys with a glassy phase and brittle crystalline or quasicrystalline precipitates exhibit no yielding and strain hardening during room temperature deformation[7,8] which limits the range of possible applications. Recently, Hays *et al.* developed a Zr–Ti–Nb–Cu–Ni–Be bulk metallic glass *in-situ* composite by coupling a high-strength glassy phase with a ductile dendritic bcc β-Ti phase.[9] This significantly improves the deformation behavior of the composite compared to the monolithic glass. However, no such composite formation has been reported for Be-free bulk metallic glass-forming alloys so far. Consequently, the aim of this work was to develop a Be-free Zr-based metallic *in-situ* composite with glass matrix and ductile bcc precipitates. This paper presents results for the phase formation, the microstructure and the thermal stability of such a $Zr_{66.4}Nb_{6.4}Cu_{10.5}Ni_{8.7}Al_8$ bulk metallic glass matrix alloy which forms a bcc phase during slow cooling. First data for the room temperature deformation of the composite will also be given.

An ingot of nominal composition $Zr_{66.4}Nb_{6.4}Cu_{10.5}Ni_{8.7}Al_8$ was prepared by arc melting under a Ti-gettered argon atmosphere. From this master alloy, bulk samples with 3 and 5 mm diameter and 50 mm length were prepared by injection casting into a copper mold in a purified argon atmosphere. An oxygen impurity level of 0.08 at % for the cylinders was determined by hot carrier gas extraction. The structure of as-prepared and annealed samples was analyzed by x-ray diffraction (XRD) with Cu K_α radiation, optical microscopy and transmission electron microscopy (TEM) coupled with energy-dispersive x-ray analysis (EDX). The thermal stability was examined by differential scanning calorimetry (DSC) in a flowing argon atmosphere (heating rate 40 $Kmin^{-1}$). The DSC was also used for the annealing treatment of the samples. Room-temperature compression tests were carried out with an electromechanical testing device under quasistatic loading (strain rate of 5×10^{-5} to 1×10^{-4} s^{-1}).

Figure 1 shows the DSC scan of the 3 mm diameter bulk sample. A glass transition with onset at $T_g=677$ K and several exothermic events indicating different steps of crystallization are observed. The onset temperatures of the first two exothermic reactions T_{x1} and T_{x2} are 713 and 755 K, respectively. To elucidate the phase formation upon primary crystallization, the sample was constant-rate heated at 40 $Kmin^{-1}$ to 725 K in the DSC, i.e., to a temperature above the first transformation peak of the DSC trace.

The XRD patterns of the as-cast and annealed state of the samples are shown in Fig. 2. The as-prepared state [Fig. 2(a)] exhibits crystalline peaks superimposed on the diffuse maxima of the amorphous phase. The diffraction peaks with maxima at $2\Theta=36.33°$, 52.23°, 65.37°, and 77.15° are identified as a β-Ti phase with bcc structure and a lattice param-

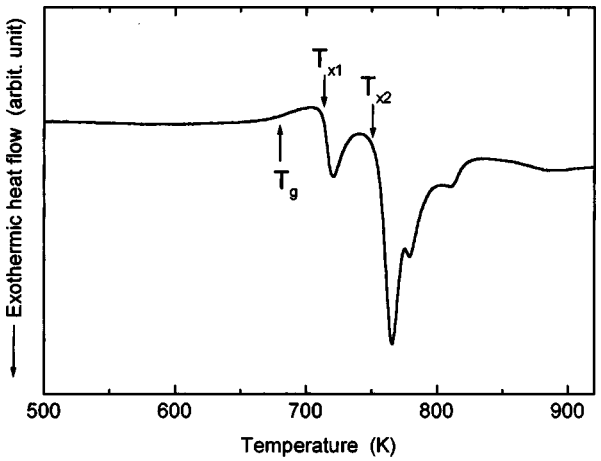

FIG. 1. DSC scan for the as-cast $Zr_{66.4}Nb_{6.4}Cu_{10.5}Ni_{8.7}Al_8$ glass matrix composite (heating rate 40 $Kmin^{-1}$).

[a]Electronic mail: u.kuehn@ifw-dresden.de

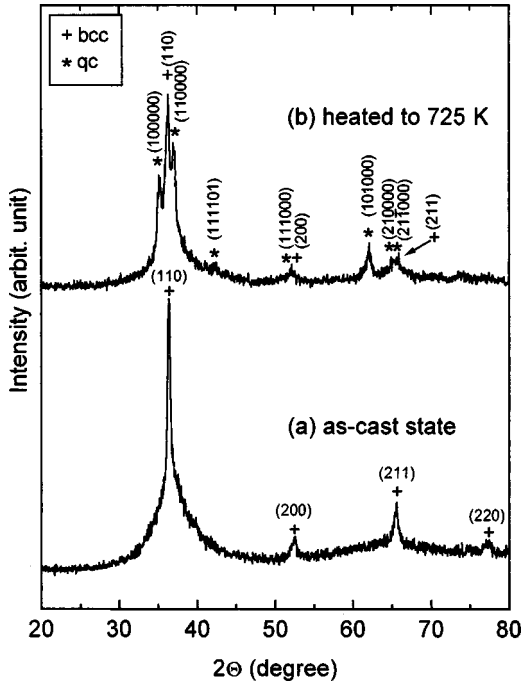

FIG. 2. XRD patterns for (a) the as-cast bulk $Zr_{66.4}Nb_{6.4}Cu_{10.5}Ni_{8.7}Al_8$ glass matrix composite, and (b) for a bulk specimen after constant-rate heating to 725 K at 40 $Kmin^{-1}$.

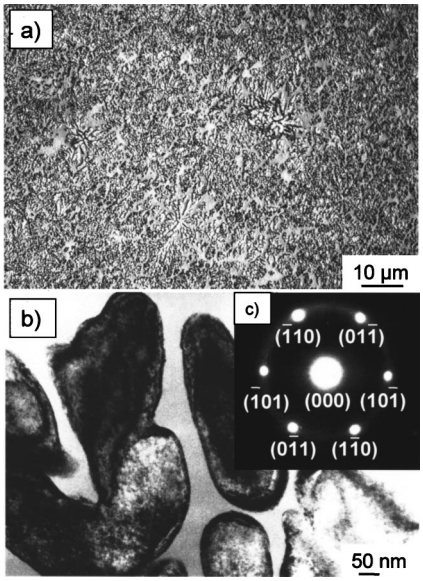

FIG. 3. Optical micrograph (a) and bright-field TEM image (b) showing the center area of an as-prepared 3-mm-diameter $Zr_{66.4}Nb_{6.4}Cu_{10.5}Ni_{8.7}Al_8$ cylinder. The selected-area diffraction pattern (c) taken along the [111] zone axis of one of the dendrites corroborates the formation of a bcc phase.

eter $a=0.3494\pm0.0004$ nm which is almost identical to the lattice parameter of 0.3496 nm found for the bcc phase in the Zr–Ti–Nb–Cu–Ni–Be *in situ* composite.[9]

Figure 2(b) displays the x-ray pattern for the sample heated to 725 K, revealing the simultaneous appearance of the bcc phase, which already exists in the as-prepared sample, together with a rather strong double peak and several weaker peaks of a quasicrystalline phase which can be indexed in icosahedral notation.[10] The quasilattice constant was determined as $a=0.4825\pm0.0001$ nm. Hence, the first exothermic DSC event corresponds to crystallization of the metallic glass matrix into an icosahedral phase.

Optical microscopy on the bulk cylinders reveals that the distribution of the bcc phase in the glass is influenced by the local cooling rate. The outermost area of the cylinders of about 100 μm thickness is almost completely amorphous. The next 300 μm are characterized by a gradually increasing volume fraction of the dendritic bcc phase. The microstructure of the center of the cylinder [Fig. 3(a)] is dominated by a high density of the dendritic β-phase precipitates embedded in the residual amorphous phase. From TEM images such as the one exemplified in Fig. 3(b) the length of the primary dendrite axes and the radius are determined to be about 2–6 μm and 200–400 nm, respectively. There is no marked change in the size of dendrites over the cross section. The selected-area electron diffraction pattern of the dendritic β-phase [Fig. 3(c)] taken along the [111] zone axis corroborates the formation of a bcc phase.

Table I compares the nominal composition of the alloy with the average compositions of the different phases as determined by EDX. The composition of the dendritic β-Ti phase strongly deviates from the nominal composition. This phase is depleted in Ni and enriched in Zr, Nb, and Al. In contrast, the composition of the amorphous phase close to the outer surface and in the center of the cylinder are relatively close to the nominal composition of the alloy, the Cu content being 2–3 at. % higher and the Nb content about 1 at. % lower. Moreover, the composition of the outermost amorphous region of the cylinder differs from that of the amorphous matrix in the center of the sample. This indicates that the composition of the amorphous phase changes upon precipitation of the bcc phase, suggesting that the solidification of the melt occurs in several steps. First, the melt in the outermost region of cylinder freezes into a glass with a composition close to the nominal one, because of the high enough cooling rate for complete glass formation near the mold. No bcc-type dendrites form in this region. For a lower cooling rate towards the center of the sample, the element niobium, which has the highest melting point of the alloying elements, triggers precipitation of bcc dendrites, due to the fact that ZrNb alloys tend to form a bcc phase.[11] Finally, upon formation of the bcc phase the residual melt depletes in Zr and Nb and becomes enriched in Cu and Ni towards a concentration where the solidification of the residual melt into a glass is favored. Therefore, the bcc phase and the glass coexist in this region.

The formation of the glass and of the bcc phase in this alloy system strongly depends on the composition and the actual cooling rate. Already small changes in composition (e.g., 1 at. % Al) or in cooling rate lead to precipitation of a second unknown crystalline phase or of quasicrystals in the center of the cylinder in addition to the bcc phase (e.g., as-

TABLE I. EDX analysis of the different phases compared to the nominal composition of the alloy.

	Alloying components (at. %)				
	Zr	Nb	Cu	Ni	Al
Nominal composition	66.4	6.4	10.5	8.7	8
Glassy phase (outermost region)	65.2	4.9	12.3	9.8	7.8
Glassy phase (center)	63.8	5.4	13.5	8.3	8.9
β-Ti phase dendrites	74.5	7.7	7.3	1.1	9.3

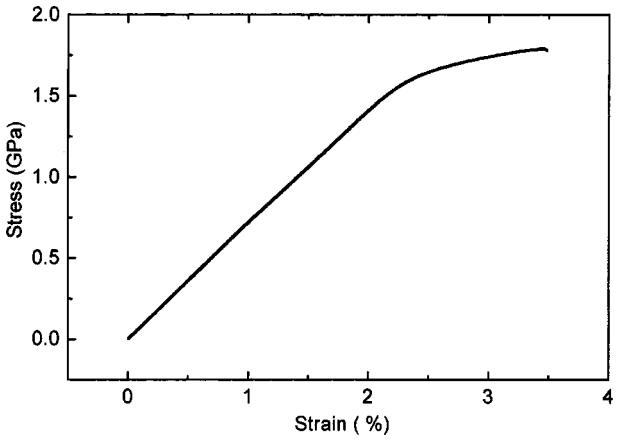

FIG. 4. Room-temperature compressive stress-strain curve for an as-cast $Zr_{66.4}Nb_{6.4}Cu_{10.5}Ni_{8.7}Al_8$ bulk cylinder.

cast $Zr_{67.4}Nb_{6.4}Cu_{10.5}Ni_{8.7}Al_7$ alloy exhibits a similar XRD pattern as the annealed $Zr_{66.4}Nb_{6.4}Cu_{10.5}Ni_{8.7}Al_8$) specimen shown in Fig. 2(b). This indicates that the tendency of formation of the glass, the quasicrystalline and the bcc phase are closely correlated. The fact that the residual glassy phase of the cylinder precipitates quasicrystals in the first step of crystallization corroborates the assumption that the alloy system reacts very sensitively to small modifications in chemical composition, cooling rate/heating rate, etc.

First room temperature compression tests reveal that the *in-situ* composite undergoes work hardening and plastic deformation prior to failure. As an example, Fig. 4 shows the compressive stress-strain curve for a 5.2-mm-long as-cast specimen with 3 mm diameter, prepared out of the center of a 5-mm-diameter sample. The composite exhibits a Young's modulus $Y=72$ GPa and yields at $\sigma_y=1.638$ GPa. The elasic strain limit is $\epsilon_y=2.4\%$. Upon further deformation the material shows strain hardening and a plastic strain $\epsilon_{\mathrm{pl}}=1.3\%$ due to the presence of the β-Ti phase until reaching the ultimate fracture stress $\sigma_f=1.8$ GPa. These features originate from the interaction of shear bands with the ductile dendritic precipitates[9] and are in apparent contrast to the deformation behavior of single-phase bulk metallic glasses exhibiting perfect elastic-plastic deformation without measurable strain hardening.[7,12–14]

In conclusion, the finding of an *in-situ* bcc β-Ti phase/bulk metallic glass composite for a Be-free glass-forming system opens the possibility of obtaining new high-strength and tough composite materials with high impact and fatigue resistance by combining the high strength of a metallic glass with the ability to undergo plastic deformation and work hardening supplied through the bcc-type dendritic precipitates. The formation of the bcc phase is strongly governed by the alloy composition and the cooling rate of solidification. We will report on the formation range of the bcc phase-reinforced metallic glass composite and a more detailed study of the mechanical properties of such materials elsewhere.

The authors are grateful to H. D. Bauer, M. Frey, H. Kempe, H. J. Klauss, B. Opitz, S. Schinnerling, and A. Voß for technical assistance and to W. L. Johnson, C. C. Hays and F. Schurack for stimulating discussions.

[1] A. Inoue, T. Zhang, and T. Masumoto, Mater. Trans., JIM **31**, 177 (1990).
[2] A. Peker and W. L. Johnson, Appl. Phys. Lett. **63**, 2342 (1993).
[3] X. H. Lin and W. L. Johnson, J. Appl. Phys. **78**, 6514 (1995).
[4] X. H. Lin, W. L. Johnson, and W. K. Rhim, Mater. Trans., JIM **38**, 474 (1997).
[5] A. Gebert, K. Mummert, J. Eckert, L. Schultz, and A. Inoue, Mater. Corros. **48**, 293 (1997).
[6] A. Inoue, Mater. Sci. Eng., A **267**, 171 (1999).
[7] A. Leonhard, L. Q. Xing, M. Heilmaier, A. Gebert, J. Eckert, and L. Schultz, Nanostruct. Mater. **10**, 805 (1998).
[8] W. L. Johnson, Mater. Sci. Forum **225**, 35 (1996).
[9] C. C. Hays, C. P. Kim, and W. L. Johnson, Phys. Rev. Lett. **84**, 2901 (2000).
[10] P. A. Bancel, P. A. Heiney, P. W. Stephens, A. I. Goldmann, and P. M. Horn, Phys. Rev. Lett. **54**, 2422 (1985).
[11] T. B. Massalski, H. Okamoto, P. R. Subramanian, and L. Kacprzak, *Binary Alloy Phase Diagrams 3*, 2nd edition (ASM International, Materials Park, OH, 1990), p. 2788.
[12] A. Inoue, T. Zhang, and T. Masumoto, Mater. Trans., JIM **36**, 391 (1995).
[13] H. A. Bruck, T. Christman, A. J. Rosakis, and W. L. Johnson, Scr. Metall. Mater. **30**, 429 (1994).
[14] C. C. Hays, C. P. Kim, and W. L. Johnson, Mater. Sci. Forum **312**, 469 (1999).